Journal of Inorganic Biochemistry 248 (2023) 112345

Contents lists available at ScienceDirect

Journal of Inorganic Biochemistry

journal homepage: www.elsevier.com/locate/jinorgbio

Cobalt(III)-py$_2$en systems as potential carriers of β-ketoester-based ligands

Marcos V. Palmeira-Mello [a,b,c], Ana B. Caballero [c,d,*], Piedad Herrera-Ramírez [c], Analu R. Costa [a], Savyo S. Santana [b], Guilherme P. Guedes [b], Amparo Caubet [c], Alzir Azevedo Batista [a], Patrick Gamez [c,d,e], Mauricio Lanznaster [b,**]

[a] Departamento de Química, Universidade Federal de São Carlos (UFSCar), 13561-901 São Carlos, São Paulo, Brazil
[b] Instituto de Química, Universidade Federal Fluminense, Outeiro S. João Batista S/N, 24020−141 Niterói, RJ, Brazil.
[c] nanoBIC, Departament de Química Inorgànica i Orgànica, Secció Química Inorgànica, Facultat de Química, Universitat de Barcelona, Martí i Franquès 1−11, 08028 Barcelona, Spain
[d] Institute of Nanoscience and Nanotechnology (IN2UB), Universitat de Barcelona, 08028 Barcelona, Spain
[e] Catalan Institution for Research and Advanced Studies (ICREA), Passeig Lluís Companys 23, 08010 Barcelona, Spain

ARTICLE INFO

Keywords:
Cobalt(III) complexes
β-Ketoester
Prodrugs
Hypoxia-activated drug delivery
Anticancer drugs
DNA binding

ABSTRACT

Two cobalt(III) complexes containing different β-ketoesters, namely [Co^{III}(**L1**)(py$_2$en)](ClO$_4$)$_2$·H$_2$O (**1**) and [Co^{III}(**L2**)(py$_2$en)](ClO$_4$)$_2$ (**2**) (py$_2$en = *N,N′*-bis(pyridin-2-ylmethyl)ethylenediamine; **L1**$^-$ = methylacetoacetate; **L2**$^-$ = ethyl 4-chloroacetoacetate) have been prepared and investigated as prototypes of bioreductive prodrugs. The presence of β-ketoester and py$_2$en ligands in **1** and **2**, as well as the perchlorate counterions, was supported by IR spectroscopy and CHN elemental analysis. The composition molecular structure of both complexes was confirmed by NMR spectroscopy and ESI mass spectrometry. Structural information was also obtained for **2** *via* X-ray diffraction analysis. The redox properties indicate that **1** and **2** are suitable for reduction under biological conditions. Investigation of DNA-interacting suggest that **1** and **2** bind DNA *via* electrostatic forces. Both complexes may be employed as possible platforms for the delivery of biologically active compounds, since their reaction with ascorbic acid in PBS at pH 6.2 and 7.4 at 37°C results in the release of the β-ketoester ligands upon Co(III)/Co(II) reduction.

1. Introduction

Hypoxic regions in tumors play a central role in cancer therapy. Dioxygen deficiency favors an adapted metabolism of cancer cells, which is related to alterations in cell cycle, metastasis and resistance to chemotherapeutic drugs [1–3]. Despite being a common obstacle to cancer treatment, hypoxia can be exploited for the selective activation of a prodrug into the tumor microenvironment [4]. Thus, different classes of prodrugs have been developed using hypoxic tissues as a target to improve the chemotherapeutic selectivity [5], highlighting those based on cobalt(III) coordination compounds [6–8].

The rationale of cobalt-based hypoxia-activated prodrugs (HAPs) involves the deactivation of cytotoxic molecules upon their coordination to a cobalt(III) complex. Highly inert complexes ($t_{2g}^6e_g^0$) can be selectively activated in hypoxic areas, releasing the coordinated drug after reduction to more labile cobalt(II) species (t_{2g}^5 e_g^2). In normoxic tissues, O_2 stabilizes cobalt(III) species, inhibiting undesired dissociation reactions and consequent drug activation. Therefore, HAPs can be designed to target the hypoxic environment of solid tumors, enhancing effectiveness, and avoiding undesired effects of widespread cytotoxicity [9–20].

Cobalt(III) complexes containing bidentate O-donor ligands present

Abbreviations: AA, ascorbic acid; acac, acetylacetonate; bzac, 1-Phenyl-1,3-butanedionate; CD, circular dichroism; ct-DNA, calf thymus DNA; CT, charge transfer; CV, cyclic voltammetry; DMF, dimethylformamide; DMSO, dimethyl sulfoxide; EB, ethidium bromide; GSH, glutathione; LMCT, ligand to metal charge transfer; MeCN, acetonitrile; naac, 1-methyl-3-(2-naphthyl)-propane-1,3-dionate; NADH, reduced nicotinamide adenine dinucleotide; PBS, phosphate buffer saline; Py$_2$en, *N, N′*-bis(pyridin-2-ylmethyl)ethylenediamine; SHE, standard hydrogen electrode; SWV, square wave voltammetry; TBAClO$_4$, tetrabutylammonium perchlorate; TBE, tris–borate–EDTA; TCEP, tris(2-carboxyethyl)phosphine; tpa, tris(2-pyridylmethyl)amine; tren, tris(2-aminoethyl)amine.

* Corresponding author at : nanoBIC, Departament de Química Inorgànica i Orgànica, Secció Química Inorgànica, Facultat de Química, Universitat de Barcelona, Martí i Franquès 1−11, 08028 Barcelona, Spain.
** Corresponding author.
E-mail addresses: ana.caballero@ub.edu (A.B. Caballero), ml@id.uff.br (M. Lanznaster).

https://doi.org/10.1016/j.jinorgbio.2023.112345
Received 18 May 2023; Received in revised form 14 July 2023; Accepted 27 July 2023
Available online 2 August 2023

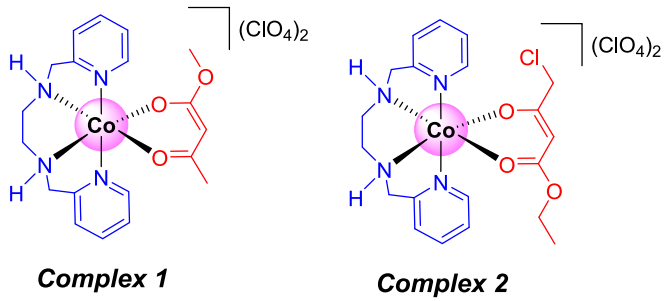

Fig. 1. Chemical structure of the complexes [Co(**L1**)(py$_2$en)](ClO$_4$)$_2$ (**1**) and [Co(**L2**)(py$_2$en)](ClO$_4$)$_2$ (**2**) (py2en = *N,N′*-bis(pyridin-2-ylmethyl)ethylenediamine; **L1** = methylacetoacetate; **L2** = ethyl 4-chloroacetoacetate).

a high stability in solution and have been investigated as potential hypoxia-selective prodrugs [21–26]. In an attempt to evaluate the efficacy of such systems, Hambley and co-workers studied some cobalt(III) complexes with β-diketone ligands [21]. Hence, the redox behavior of the complex [Co(acac)(tpa)](ClO$_4$)$_2$ (acac = acetylacetonate, tpa = tris (2-pyridylmethyl)amine) was investigated and compared to the non-acac analogues [Co(bzac)(tpa)](ClO$_4$)$_2$ and [Co(naac)(tpa)](ClO$_4$)$_2$ (bzac = 1-phenyl-1,3-butanedionate, naac = 1-methyl-3-(2-naphthyl)-propane-1,3-dionate). The complex containing the acac ligand presented a more negative cathodic peak potential (E_{pc} = −605 mV *vs.* Fc/Fc$^+$) than those containing bzac and naac (E_{pc} = −560 mV *vs.* Fc/Fc$^+$). These electrochemical data in DMF revealed that replacement of methyl with benzyl or naphthyl groups favors cobalt(III) reduction, showing the influence of the electron density over the metal center. In addition, fluorescence measurements in methanol-water solution indicated the dissociation of [Co(naac)(tpa)](ClO$_4$)$_2$ upon reduction by an excess of ascorbic acid (AA) [21].

Recently, Mathuber and co-workers synthesized several (EGFR-inhibitor)-containing cobalt(III) prodrugs (EGFR = epidermal growth factor receptor) and investigated the role played by the electron-donating methyl group of the acac ancillary ligands [25]. Cyclic voltammetry experiments in aqueous solution revealed that the methylation at [Co(Meacac)$_2$L]$^+$ (L = EFGR-inhibitor ligand) resulted in a E_{pc} of 4 mV *vs.* NHE, a lower value compared to that of the non-methylated analogue [Co(acac)$_2$L]$^+$ (62 mV *vs.* NHE). Reactions with AA, glutathione (GSH) and reduced nicotinamide adenine dinucleotide (NADH) at pH 7.4 indicated that all biological reducing agents were not able to reduce the metal center that would release the free EGFR inhibitor. However, the time-dependent release of this ligand was observed by HPLC-MS analysis, after incubation in fetal calf serum pH 7.4 at 37°C. Thus, 43% and ~ 85% of the initial [Co(Meacac)$_2$L]$^+$ and [Co(acac)$_2$L]$^+$ species were detected, after 26 h, in agreement with cyclic voltammetry results, highlighting the effect of the methyl group on the acac ligand.

In an attempt to explore a new bioreductive platform for drug delivery, we investigated new cobalt(III)-β-ketoester complexes. Esterification of a drug will alter its properties, and its pharmacokinetic profile may be affected [27–29]. Such compounds represent common prodrugs that can be activated through hydrolysis by esterases, which are overexpressed in tumors. Additionally, in a hypoxic environment, a labile cobalt(II) complex can be obtained *in situ* upon Co(III)/Co(II) reduction, releasing the β-ketoester ligand acting as a drug. In this context, the development of Co(III)-β-ketoester complexes can be exploited in an attempt to provide more selective chemotherapeutic agents, targeting cancer cells [28].

In the present work, we report on the synthesis and characterization of two new cobalt(III) complexes, namely [Co^{III}(**L1**)(py$_2$en)](ClO$_4$)$_2$·H$_2$O (**1**) and [Co^{III}(**L2**)(py$_2$en)](ClO$_4$)$_2$ (**2**) (py$_2$en = *N,N′*-bis (pyridin-2-ylmethyl)ethylenediamine; **L1**$^-$ = methylacetoacetate; **L2**$^-$ = ethyl 4-chloroacetoacetate) (Fig. 1). Py$_2$en auxiliary ligand was chosen due to its ability to bind to metal center *via* tetradentate mode, modulating its redox potential. Hence, solution studies under a reducing microenvironment (to mimic a hypoxic condition) were performed for both complexes to observe the potential release of the β-ketoester moiety. Furthermore, DNA-binding studies were also conducted.

2. Experimental

2.1. Materials and instrumentation

All reagents and solvents, including ligands **HL1** and **HL2**, were purchased from commercial sources and used without further purification. The ancillary ligand py$_2$en was prepared as previously described [30,31]. Infrared spectra were recorded on a Varian 600 FTIR equipped with a Pike ATR Miracle accessory (diamond/ZnSe crystal, resolution: 4 cm^{-1}). UV–Visible spectra were recorded in spectroscopic grade solvents and aqueous buffered solutions, using a Varian Cary 50 spectrophotometer, using a 1 cm path length quartz cuvette. ^{1}H (400 MHz), ^{13}C {^{1}H} (100.62 MHz), HSQC and HMBC 2D NMR spectra were recorded on a 9.4 T Bruker Avance III 400 MHz spectrometer, using DMSO-d_6 as solvent. Chemical shifts (δ) are given in ppm and coupling constants (*J*) in hertz (Hz). Elemental analyses were performed with a Perkin-Elmer CHN 2400 micro analyzer at the University of São Paulo (USP, Brazil). ESI-MS spectra were obtained by direct infusion using a Perkin Elmer SQ-300 mass spectrometer, using acetonitrile (MS grade) as solvent. Electrochemical experiments were performed in MeCN and PBS/DMSO solutions (HPLC grade) with a BASi Epsilon Potentiostat-Galvanostat at room temperature under argon atmosphere. The experiments were conducted in acetonitrile (HPLC grade) containing 0.1 M tetrabutylammonium perchlorate (TBAClO4) as supporting electrolyte, and in aqueous PBS solutions at pH 7.4 and at pH 6.2. A standard three-component system was used: a glassy carbon working electrode, a platinum wire auxiliary electrode, and an Ag/AgCl reference electrode. A BASi non-aqueous Ag/AgCl electrode kit (PN MF-2064) was used for measurements in acetonitrile, while a standard BASi 3 M NaCl (PN MF-2056) was used for PBS solutions. Ferrocene (Fc/Fc$^+$) was used as an internal reference for the measurements in acetonitrile (E° = 0.4 V *vs* SHE) [32]. The potentials in aqueous PBS solutions, reported *versus* SHE (standard hydrogen electrode), were calculated by adding 0.209 V to the values *versus* the standard Ag/AgCl electrode [33]. For the biological studies, sodium cacodylate, Tris–borate–EDTA 1× (TBE), calf thymus DNA (ct-DNA), ethidium bromide (EB, 10 mg mL^{-1} solution) and Hoechst 33258 were purchased from Sigma Aldrich. pBR322 plasmid DNA (4361 bp, 0.5 μg mL^{-1}) was purchased from Thermo Scientific. SYBR™ Safe DNA Gel Stain was purchased from Invitrogen. All chemicals were used without further purification. Ultrapure Milli-Q® water was used to prepare the solutions.

2.2. Synthesis of the complexes

The ancillary ligand py$_2$en and the precursor [CoCl$_2$(py$_2$en)]ClO$_4$ were obtained as described previously [15,34]. The complexes [Co^{III}(**L1**)(py$_2$en)](ClO$_4$)$_2$·H$_2$O (**1**) and [Co^{III}(**L2**)(py$_2$en)](ClO$_4$)$_2$ (**2**) were synthesized according to the following general procedure. A methanolic solution of **HL1** or **HL2** (0.2 mmol, 10 mL) containing 34 μL of Et$_3$N was added to a methanolic solution of [Co(py$_2$en)Cl$_2$]ClO$_4$ (0.2 mmol, 10 mL). The mixture was refluxed for 1 h and subsequently cooled to room temperature. Then, 0.4 mmol of LiClO$_4$ was added and the reaction was kept under stirring for further 30 min in an ice bath. Complexes **1** and **2** were isolated by filtration as pale pink solid powders, washed with cold methanol, and dried under reduced pressure.

[Co(**L1**)(py$_2$en)](ClO$_4$)$_2$·H$_2$O (**1**). Yield 45%. (ATR, ν_{max}/ cm^{-1}): 3224 (N − H); 2983 (C − H); 1594 (C=O); 1500–1400 (C=C, C=N); 1289 (C − O); 1095 (Cl − O). Anal. Calc. for C$_{19}$H$_{27}$Cl$_2$CoN$_4$O$_{12}$: C, 36.04; H, 4.30; N, 8.85%. Found: C, 35.67; H, 4.22; N, 8.69. %. ESI-MS (MeCN): m/z^+ = 208.3, 100% for [Co(**L1**)(py$_2$en)]$^{2+}$.^{1}H NMR (400 MHz, DMSO-d_6, δ ppm): 8.33–8.22 (m, 4H, H4, H6), 8.18 (s, 1H, NH),

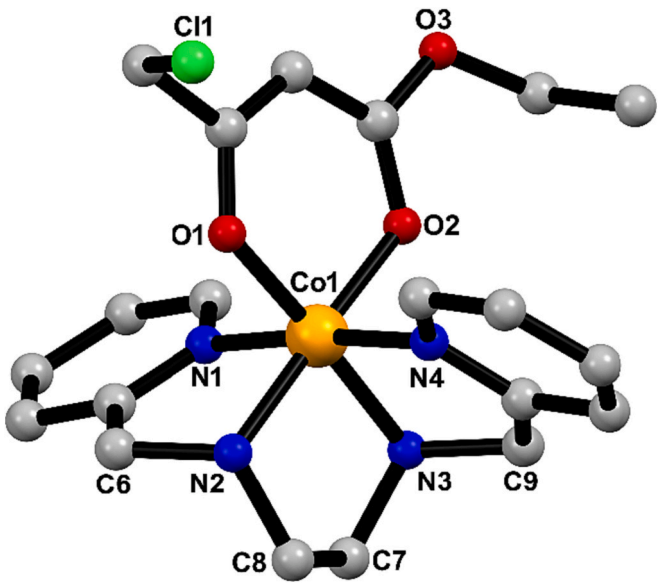

Fig. 2. View of the mononuclear cationic $[Co^{III}(L2)(py2en)]^{2+}$ species in **2**. Hydrogen atoms and counterions were omitted for sake of clarity. Color codes: C (gray), N (blue), Co (orange), Cl (green) and O (red). (For interpretation of the references to color in this figure legend, the reader is referred to the web version of this article.)

7.96 (s, 1H, NH), 7.84–7.73 (m, 4H, H3, H5), 5.01 (s, 1H, H3'), 5.00–4.84 (m, 2H, H1a), 4.32 (d, J = 17.4 Hz, 1H, H1a), 4.14 (d, J = 17.4 Hz, 1H, H1a), 3.85 (s, 3H, H5'), 2.61 (m, 4H, H1b), 2.09 (s, 3H, H1'). ^{13}C NMR (101 MHz, DMSO-d_6, δ ppm): 189.9, 171.8, 164.1, 163.7, 150.7, 150.6, 141.3, 125.3, 125.2, 123.4, 123.2, 83.6, 59.2, 58.9, 53.7, 53.1, 26.6.

[Co(**L2**)(py$_2$en)](ClO$_4$)$_2$ (**2**). Yield 50%. IR (ATR, ν_{max}/ cm^{-1}): 3205 (N – H), 2983 (C – H); 1593 (C=O); 1500–1400 (C=C, C=N); 1284 (C – O); 1090 (Cl – O). Anal. Calc. for $C_{20}H_{26}Cl_3CoN_4O_{11}$: C, 36.19; H, 3.95; N, 8.44%. Found: C, 36.09; H, 3.96; N, 8.18%. ESI-MS (MeCN): m/z^+ = 232.2, 100% for $[Co(\mathbf{L2})(py_2en)]^{2+}$. ^{1}H NMR (400 MHz, DMSO-d_6, δ ppm): 8.41 (d, J = 6.1 Hz, 1H, H6), 8.32–8.23 (m, 3H, H6c, H4, H4c), 8.20 (s, 1H, NH), 8.05 (s, 1H, NH), 7.84 (d, J = 7.9 Hz, 2H, H3 and H3c), 7.78 (t, J = 6.1 Hz, 2H, H5, H5c), 5.23 (s, 1H, H3'), 4.93 (dd, J = 17.4, 6.6 Hz, 1H, H1a), 4.85 (dd, J = 17.4, 6.3 Hz, 1H, H1c), 4.49–4.26 (m, 4H, H1a, H1' and H5'), 4.22 (d, J = 12.3 Hz, 1H, H5'), 4.13 (d, J = 17.4 Hz, 1H, H1c), 2.49 (m, 4H, H1b), 1.16 (t, J = 7.1 Hz, 3H, H6'). ^{13}C NMR (101 MHz, DMSO-d_6, δ ppm): 183.40, 172.5, 164.0, 163.5, 150.9, 150.7, 141.5, 141.4, 125.4, 125.3, 123.5, 123.4, 84.5, 63.4, 59.3, 59.1, 53.7, 53.3, 45.5, 13.9.

2.3. Single crystal X-ray diffraction

Single crystals of **2** were obtained from recrystallization in methanol. X-ray diffraction data was collected on a Bruker D8 Venture diffractometer using Mo Kα radiation (λ = 0.71073 Å) at room temperature. Data collection, cell refinement and data reduction were performed using Bruker Instrument Service, APEX3 [35] and SAINT [36], respectively. The absorption correction using equivalent reflections was done with the SADABS program [37]. The structure solution and full-matrix least-squares refinement based on F^2 was carried out with SHELXS and SHELXL programs [38]. All atoms except hydrogens were refined anisotropically and hydrogen atoms were treated using a constrained refinement. Structure drawings were generated by Mercury program [39]. A summary of the crystal, data collection and refinement is gathered in Table S3. Fig. 2 shows the thermal ellipsoids for **2**. CCDC 2244204 contains the supplementary crystallographic data for this paper, which can be obtained from The Cambridge Crystallographic Data Centre *via* https://summary.ccdc.cam.ac.uk/structure-summary-form.

2.4. Reactivity assays – Ligand release studies

Ligand dissociation of complexes **1** and **2** was investigated before and after reaction with ascorbic acid (AA). Fresh stock solutions of the complexes (5.0 mM) were prepared in DMSO. For the reactivity experiments with the reducing agent, aliquots of the stock solutions of the complexes were diluted with PBS (pH 6.2 and 7.4) to 0.5 mM. A final concentration of 5.0 mM of AA was used. The final solutions were prepared (i) in open air and (ii) purged with argon or dioxygen. For the last one, solutions of complexes were added to the quartz cuvettes, which were kept sealed. The cuvettes were purged during 15 min and then, the solution containing the reducing agent was transferred with a needle into the cuvette. The monitoring of UV–Vis spectra was carried out using a Varian Cary 50 spectrophotometer with an 18-multicell accessory in 1 cm quartz cuvettes and monitored by 24 h at 4800 nm min^{-1} at 37°C. Conversion rates were estimated by measuring the absorbance variations of the complexes at 498 nm during two different timescales (6 h and 24 h period). Absorbance spectra of the complexes were also recorded before the start of the reactions (corresponding to 0% conversion) and at the end of the reaction (corresponding to 100% conversion).

2.5. DNA-binding studies

For the DNA-binding studies, the concentration of calf thymus DNA (ct-DNA) was determined spectrophotometrically at 260 nm using the nucleobase molar absorptivity of 6600 M^{-1} cm^{-1}. The absorbance ratio at 260 and 280 nm (A_{260}/A_{280}) of 1.90 indicated that the DNA was sufficiently free of protein [40,41].

2.5.1. UV–Vis measurements

The UV–Visible spectra were obtained from cacodylate/NaCl buffer solutions (1 mM sodium cacodylate, 20 mM NaCl, pH 7.3) using a Varian Cary 100 spectrophotometer at room temperature, with a 1 cm path length quartz cuvette. The stability of 25 μM solutions of complexes **1** and **2** in 1 mM cacodylate – 20 mM NaCl buffer (containing 1% DMSO) solution was previously monitored over a period of 24 h. After that, DNA-binding measurements were performed using increasing concentrations of ct-DNA (0–100 μM) added to a 25 μM solution of the complexes in cacodylate–NaCl buffer. The intrinsic binding constant, K_b, was obtained using Eq. 1.

$$\frac{[DNA]}{(\varepsilon_a - \varepsilon_f)} = \frac{[DNA]}{(\varepsilon_0 - \varepsilon_f)} + \frac{1}{K_b(\varepsilon_0 - \varepsilon_f)} \quad (1)$$

where [DNA] is the concentration of ct-DNA in base pairs, ε_a is the extinction coefficient observed at the given DNA concentration, ε_f is the extinction coefficient of the free complex in solution, and ε_0 is the extinction coefficient of the compound when fully bound to DNA.

2.5.2. Viscosity assays

The viscosity experiments were carried out by using an Ostwald viscosimeter maintained in a thermostatic bath at 25°C. The concentration of ct-DNA in Tris-HCl was maintained constant at 80 μM. The complexes were solubilized in DMSO, and their concentrations were varied, to obtain different complex-to-DNA ratios (namely 0.0, 0.12, 0.25, 0.31, 0.37, 0.50) in the final solutions (4000 μL, DMSO 30%). The flow times (five replicates) were recorded with a digital stopwatch. The specific viscosity values $(\eta/\eta_0)^{1/3}$ were plotted *versus* [complex]/[ct-DNA], where η and η_0 correspond to the relative viscosity of DNA in the presence and the absence of the complexes, respectively. Eq. (2) was used to calculate the relative viscosity of DNA; the η_0 values were determined from the flow times of the DNA solutions (t) corrected for

the flow times of the buffer (t_0).

$$\eta 0 = \frac{(t - t0)}{t0} \quad (2)$$

2.5.3. Circular dichroism spectroscopy

Circular dichroism (CD) spectra were recorded with a JASCO-815 spectropolarimeter. Solutions of ct-DNA (100 μM) in 1 mM cacodylate – 20 mM NaCl buffer (pH 7.3) were incubated for 1 h at 37°C with different amounts of the complexes (*viz.* complex-to-DNA ratios of 0, 0.2, 0.6 and 1.0). The CD spectra were obtained at room temperature from 230 to 320 nm using a quartz cuvette with an optical path length of 0.5 cm and a scanning rate of 200 nm min^{-1}.

2.5.4. Fluorescence – Dye displacement assay

Ethidium bromide (EB)-displacement studies were carried out using a HORIBA Jobin–Yvon iHR320 spectrofluorometer. A solution of ct-DNA (15 μM_{bp}) was pre-incubated with EB (75 μM) in 1 mM cacodylate – 20 mM NaCl buffer (pH 7.3) for 30 min at 37°C, to allow full interaction of the dye with the biomolecule. Increasing amounts of **1** and **2** (0–50 μM) were subsequently added to the DNA samples, followed by incubation for 1 h. The emission spectra of all complexes were recorded at 25°C upon excitation at 514 nm.

Hoechst-displacement studies were carried out by monitoring the fluorescence of Hoechst-ct-DNA upon addition of complexes **1** and **2**. Solutions containing Hoechst (5 μM) and ct-DNA (100 μM) were prepared, mixed, and incubated for 30 min at 25°C. Next, increasing amounts of **1** and **2** (0–40 μM) were added to the Hoechst-DNA solution, and 200 μL of the resulting solution were added to an opaque 96-well plate. Fluorescence spectra were registered from 370 to 700 nm at 25, 30 and 37°C upon excitation at 343 nm using a Synergy/H1-Biotek fluorimeter. For data analysis, the classical Stern-Volmer eq. (3) was used.

$$\frac{F_0}{F} = 1 + K_{sv}\,[Q] \quad (3)$$

where F_0 and F correspond to the fluorescence intensities in the absence and presence of **1** or **2**, respectively, [Q] represents the concentration of **1** or **2** and Ksv is the Stern Volmer constant. The binding constant (K_b) was estimated using Eq. (4), and the thermodynamic parameters, ΔH, ΔS and ΔG were determined using Eqs. (5) and (6).

$$log\ \frac{F0 - F}{F} = logK_b + nlog[Q] \quad (4)$$

$$ln\frac{Kb2}{Kb1} = \left(\frac{1}{T2} - \frac{1}{T1}\right)\frac{\Delta H}{R} \quad (5)$$

$$\Delta G = -RTlnK = \Delta H - T\Delta S \quad (6)$$

where K_b is the binding constant between the complexes and the ct-DNA at different temperatures, and R is the gas constant ($R = 8.314$ J/K mol).

2.5.5. Agarose gel electrophoresis

The potential DNA-cleaving properties of the complexes were investigated using agarose gel electrophoresis. Stock solutions of **1** and **2** (10 mM) were prepared in 1 mM cacodylate – 20 mM NaCl buffer (pH 7.3). Plasmid pBR322 (15 μM_{bp}) was treated with the complexes (5, 10, 25 and 50 μM) in the absence and presence of AA (100 μM), GSH (150 μM) and tris(2-carboxyethyl)phosphine hydrochloride (TCEP; 1 mM). The samples treated with reducing agent were pre-incubated at 37°C for 30 min. Later, the samples were also incubated at 37°C for 1.5 h. Then, 4 μL of loading buffer (30% glycerol, 5 mM xylene cyanol) were added and the samples were electrophoresed in TBE 1× at 6.5 Vcm^{-1} for 1 h in a BioRad horizontal tank. Next, the gel was stained with SYBR™ Safe overnight, and the images were acquired using a Gel Doc EZ Imager instrument (Bio-Rad). The DNA-cleaving complex $[Cu(phen)_2(H_2O)](NO_3)_2$, also known as Sigman's reagent, was used as a reference compound [42].

Table 1
Selected bond lengths (Å) and angles (°) for compound **2**.

Bond lengths		Bond angles	
Co1-O1	1.886(2)	O1-Co1-O2	95.6(1)
Co1-O2	1.899(2)	O1-Co1-N1	90.0(1)
Co1-N1	1.927(3)	O1-Co1-N2	86.9(1)
Co1-N2	1.927(3)	O1-Co1-N3	175.3(1)
Co1-N3	1.938(3)	O1-Co1-N4	93.1(1)
Co1-N4	1.926(4)	O2-Co1-N1	93.5(1)
N2-C6	1.489(6)	O2-Co1-N2	177.1(1)
N2-C8	1.488(5)	O2-Co1-N3	88.8(1)
N3-C7	1.488(5)	O2-Co1-N4	90.4(1)
N3-C9	1.486(7)	N1-Co1-N2	85.2(1)
C7-C8	1.511(6)	N1-Co1-N3	91.5(1)
C20-Cl1	1.745(8)	N2-Co1-N3	88.7(1)
		N2-Co1-N4	90.7(1)
		N3-Co1-N4	85.2(1)

3. Results and discussion

3.1. Synthesis, infrared spectroscopy, and X-ray crystallography

The cobalt(III) complexes **1** and **2** were synthesized by substitution of the chlorido ligands from the precursor compound $[CoCl_2(py_2en)]ClO_4$ with methylacetoacetate and ethyl 4-chloroacetoacetate, respectively, in the presence of Et_3N. The products of the reactions were isolated as pale pink solids, and their compositions were confirmed by CHN elemental analyses. For both complexes, the IR spectra (Figs. S1 and S2) show the presence of bands at ≈1289 cm^{-1} and ≈1593 cm^{-1} assigned, respectively, to the C—O and C═O bonds of β-ketoester ligands [43].

Suitable single crystals for X-ray diffraction were obtained by slow evaporation of methanolic solution. Compound **2** crystallized in the $P\bar{1}$ space group and its crystal structure is comprised of one mononuclear cationic species $[Co^{III}(L2)(py_2en)]^{2+}$ (Fig. 2 and Table S1) and two perchlorates as counterions. Table 1 contains selected bond lengths and angles.

The cobalt(III) ion lies on a distorted octahedral environment, coordinated to one py_2en auxiliary ligand in a tetradentate mode, by both pyridine (N1 and N4) and secondary amine (N2 and N3) moieties, and one deprotonated β-ketoester molecule by O1 and O2 atoms. The $\mathbf{L2}^-$ coordination mode resulted in a stable six-membered chelated ring. Moreover, the py_2en pyridine rings are *cis*, while the β-ketoester oxygen atoms are trans-coordinated to the py_2en secondary amine fragments (N2 and N3). The bond angles involving the metal center vary between 85.2(1) to 177.1(1)°, as listed in Table 1. The Co—N and Co—O bond distances are in the range 1.926(4)–1.938(3) Å and 1.886(2)–1.899(2) Å, respectively, which are typical for low-spin cobalt(III) ions [13,44], as reported for others cobalt(III) complexes containing β-diketonate ligands, such as $[Co(acac)(tpa)](ClO_4)_2$, $[Co(Clacac)(tpa)](ClO_4)_2$ [21], $[Co(acac)_3]$ [45], $[Co(acac)(bpy)(N_3)_2]$, $[Co(acac)(en)(N_3)_2]$ [46], $[Co(phen)_2(acac)](ClO_4)_2$ and $[Co(dpq)_2(acac)](ClO_4)_2$ [47].

The crystal packing is stabilized by a network of hydrogen bonds and a series of C—H···O short contacts involving the mononuclear cationic complex and the perchlorate counter ions. Geometric parameters associated with these interactions are gathered in Table S2. Oxygen perchlorate atoms act as hydrogen acceptors through the interaction with the py_2en secondary amine moieties (N2—H2···O8 and N3—H3···O7). Furthermore, a second hydrogen bond connecting counter-ion and the β-diketonate hydrogen atom (C18-H18···$O5^{iv}$) leads to set of two cationic species and two perchlorates in solid state. This set of molecules is linked to the neighbouring one through C_{sp2}-H···O short contacts (C2^{ii}—H2A^{ii}···O10) (Fig. 3).

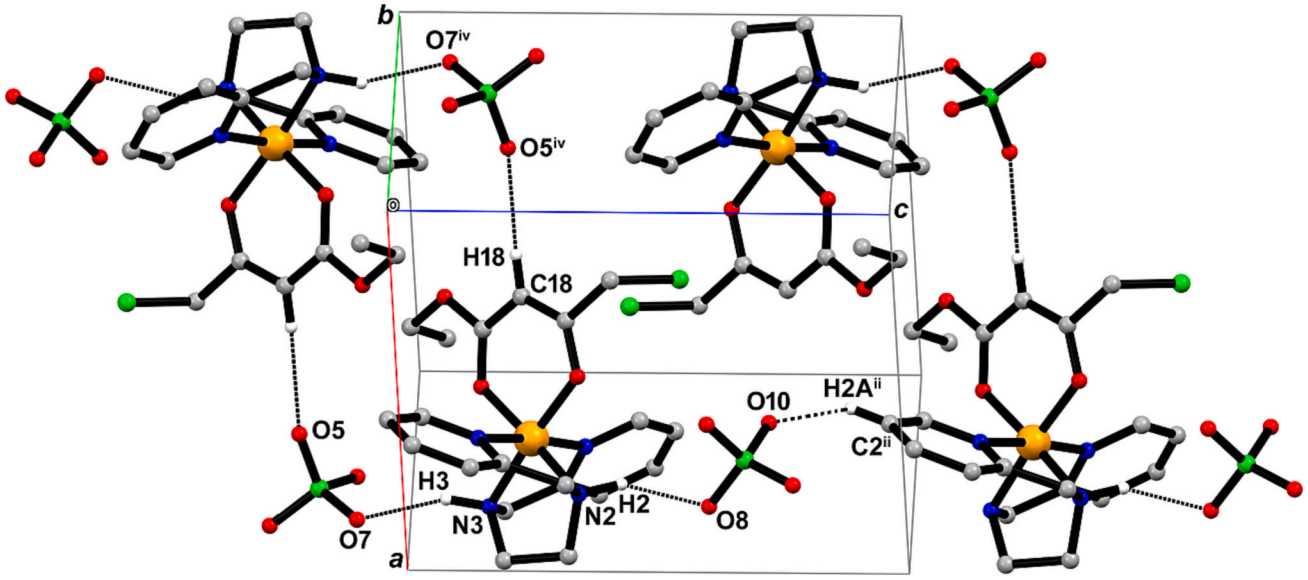

Fig. 3. Details of the crystal packing of compound **2**, showing the intermolecular hydrogen bonds (dotted lines) between the mononuclear cationic complex and the perchlorate anions. Crystallographic axis orientation is shown in the Figure.

3.2. Solution studies

The molecular structures of **1** and **2** in solution were investigated by ^{1}H and ^{13}C NMR in DMSO-d_6 (Figs. S3–S6). The chemical shift assignments were made based on COSY, HSQC and HMBC correlations and by comparison with analogous complexes [48–50]. The ^{1}H NMR spectrum of **1** shows the pyridine Hα hydrogen atoms of py$_2$en at 8.33–8.22 (m) (2H). The other aromatic hydrogen atoms are found as multiplets at 8.33–8.22 ppm (2H) and 7.84–7.73 (m) ppm (4H). The aliphatic hydrogen atoms from py$_2$en are in the range of 5.00–2.61 ppm (8H). These chemical shifts are similar to those observed for the complex [Co(py$_2$en)(TCC)]ClO$_4$ [48]. The remaining two amino hydrogen atoms are found as two singlets at 8.18 and 7.96 ppm. For complex **2**, the pyridine Hα hydrogen atoms are observed at 8.41 (d) and 8.32–8.23 ppm (m) (2H). The other pyridine hydrogen atoms are found at 8.32–8.23 (m), 7.84 (d) and 7.78 (t) ppm (6H). The aliphatic hydrogen atoms are in the range 4.93–2.49 ppm (8H) and the two –NH hydrogen atoms are observed at 8.20 (s) and 8.05 (s) ppm.

Tetradentate ligands, such as py$_2$en, can bind to a transition-metal ion in two different configurations, namely *cis*-α or *cis*-β [51,52]. The presence of a single peak for the pyridine Hα hydrogen atoms of py$_2$en for **1** and two sets of peaks for **2** indicate that these complexes adopt a *cis*-α and a *cis*-β conformation in solution, respectively [49]. The *cis*-α conformation adopted by **1** is characterized by two *trans*-coordinated pyridine rings while, for **2**, the pyridines are in *cis*-β conformation, which is different from that determined by X-ray diffraction (see Fig. 2) [53]. The Hα hydrogen atom of the β-ketoester ligand is found as a singlet at 5.01 ppm for **1** and 5.25 ppm for **2**, while the –CH$_2$ hydrogen atoms of **2** are seen at 4.49–4.26 (m) ppm. The –CH$_3$ hydrogen atoms appear as two singlets at 3.85 and 2.09 ppm for **1**, and as a triplet at 1.16 ppm for **2**. These chemical shifts are similar to those reported for an analogous β-ketoester-containing complex [50].

For **1**, the pyridine carbon atoms of py$_2$en are found in the range 164.1–123.2 ppm, and its aliphatic atoms are observed between 59.1 and 53.1 ppm. For **2**, the chemical shifts of the aromatic and aliphatic carbon atoms of py$_2$en are found at 164.0–123.4 ppm and 59.3–53.3 ppm, respectively. For the β-ketoester ligands, for complex **1**, the corresponding chemical shifts are observed at 189.9 (C=O), 171.8 (C=C–Hα), 83.6 (C–Hα), 53.7 (CH$_3$–O) and 26.6 (CH$_3$) ppm. For **2**, the β-ketoester peaks are found at 183.4 (C=C–Hα), 172.5 (C=O), 84.5 (C–Hα), 63.4 (CH$_2$–O), 45.5 (CH$_2$–Cl) and 13.9 (CH$_3$) ppm. These δ values are also in agreement with previously reported data [50].

Table 2
Electrochemical data for complexes **1** and **2** in MeCN and PBS (V *vs.* SHE) at different pH values. Ferrocene (Fc/Fc$^+$) (E° = +0.4 V *vs* SHE).

Complex	MeCN			PBS pH 6.2		PBS pH 7.4	
	CV			CV	SWV	CV	SWV
	E_{pc}	ΔE	I_{pa}/I_{pc}	E_{pc}	E_{pc}	E_{pc}	E_{pc}
1	−0.22	0.24	0.27	−0.19	−0.13	−0.19	−0.13
2	−0.14	0.18	0.29	−0.10	−0.07	−0.05	−0.04

Electrospray ionization mass spectrometry (ESI-MS) spectra of **1** and **2** in acetonitrile (Fig. S7) show the *m/z* peaks for the molecular ions of [Co(L1)(py$_2$en)]$^{2+}$ and [Co(L2)(py$_2$en)]$^{2+}$ as the main species in solution at 208.3 and 232.2, respectively.

The UV–Vis spectra of **1** and **2**, recorded in DMSO (using two different concentrations, *i.e.*, 1.0 mM and 0.1 mM) are very similar to each other (Figs. S8 and S9). The complexes present an absorption at 297 nm (**1**; ε = 5540 M^{-1} cm^{-1}) and 300 nm (**2**; ε = 5350 M^{-1} cm^{-1}), which is assigned to a mixture of intraligand π → π* and LMCT transitions. A low-energy absorption, attributed to d-d transitions, is observed at 500 nm (ε = 175 M^{-1} cm^{-1}) for **1** and at 498 nm for **2** (ε = 184 M^{-1} cm^{-1}). Moreover, for **1**, a shoulder is also seen at *ca.* 350 nm [15,34].

The stability of complexes **1** and **2** in aqueous media was investigated by monitoring their UV–Vis spectra in PBS (containing 10% DMSO) at pH 6.2 and 7.4, at 37°C (Figs. S10 and S11). No changes were observed after 24 h (at the two different concentrations), indicating that **1** and **2** are stable under these conditions.

3.3. Electrochemical behavior in solution

Structural changes of the ligands can modulate the electron density around the metal center and therefore modify the Co^{3+}/Co^{2+} redox potential. Cyclic voltammetry (CV) measurements were therefore performed for complexes **1** and **2** in acetonitrile and PBS. The cyclic voltammograms obtained in acetonitrile revealed the lack of reversibility of the Co^{3+}/Co^{2+} process, with ΔE and I_{pa}/I_{pc} values of 0.24 V and 0.27 for **1**, and 0.18 V and 0.29 for **2** (Table 2). In addition, E_{pc} values were found at −0.22 and − 0.14 V *vs.* SHE for **1** and **2**, respectively (Fig. S12). These peak potentials follow the same trend as those observed by Hambley and

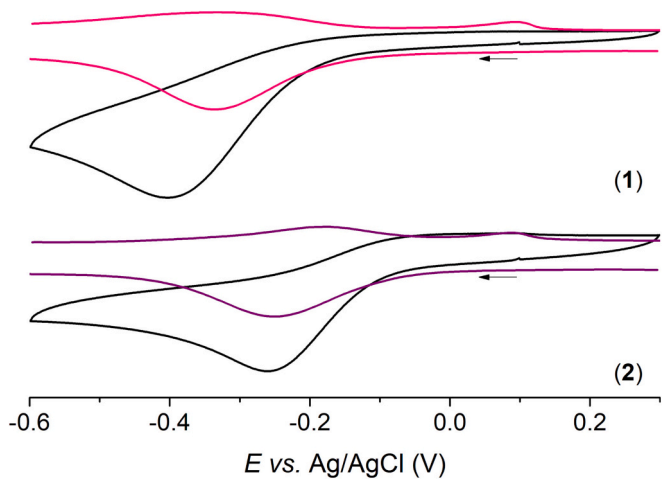

Fig. 4. Cyclic and square-wave voltammograms of complexes **1** (top) and **2** (bottom) in PBS at pH 7.4. CV at 0.1 V s^{-1} and SWV with pulses of 40 mV, step sizes of 4 mV and frequency of 15 Hz, using a three-electrode system (working: carbon; ref.: Ag/AgCl (NaCl 3 M, BASi); aux.: Pt wire).

co-workers for analogous cobalt(III)-β-diketone complexes [21]. For instance, potentials of −0.61 and − 0.52 V *vs.* Fc/Fc^+ in DMF were found for $[Co(acac)(tpa)](ClO_4)_2$ and $[Co(Clacac)(tpa)](ClO_4)_2$, respectively. Although the electrochemical data were not reported in the same solvent, they match our results, which suggest that **2** is more susceptible to Co^{3+} reduction than **1**. This difference may be explained by the electron-withdrawing effect of the chlorine atom of the β-ketoester ligand in **2**, which facilitates the Co^{3+} reduction. Such electrochemical behavior was also observed by Mathuber and co-workers with cobalt(III)-acac prodrugs [25].

As a potential bioactivation of these cobalt(III) prodrugs into a solid tumor is dependent on their reduction potential, the redox properties of **1** and **2** were investigated by CV in PBS. The peak potentials attributed to the Co^{3+}/Co^{2+} reduction follow the same trend as those obtained in acetonitrile, with a slight shift. Since the electrochemical processes of these compounds are irreversible, square-wave voltammetry (SWV) measurements were also conducted to allow a more accurate determination of the reduction potentials. The SWV studies provided comparable results and reduction potentials of −0.13 and − 0.07 V *vs.* SHE were found for **1** and **2**, respectively, at pH 6.2 (Fig. S13). These results suggest that complex activation by Co^{3+}/Co^{2+} reduction may occur under biological conditions, followed by ligand dissociation due to the liability of the cobalt(II) species [15,25,44]. It can be noted that the influence of pH on the reduction potential of **2** is minor, with a peak potential of −0.04 V *vs.* SHE at pH 7.4, which is 30 mV higher than that at pH 6.2 (Table 2 and Fig. 4).

3.4. Activation of the complexes: Ligand release

To simulate the reducing environment found in solid tumors, freshly prepared solutions of the complexes and ascorbic acid were mixed. The resulting reaction mixtures were monitored by UV–Visible spectroscopy at 37°C for 24 h, using different atmospheric conditions. Under argon, a decrease of the absorbance at 500 nm (for **1**) and 498 nm (for **2**) is observed (Fig. 5), which was used to estimate the reaction progression (%). At pH 7.4, significant transformation of the complexes were observed, with 69% and 84% conversion for **1** and **2**, respectively after 24 h (Fig. 5 and Table 3).

In the presence of dioxygen, significant spectroscopic changes were observed after long periods of time (due to the "degradation of the original compounds"). Thus, the conversion percentages (illustrating the ligand release upon Co(III)-to-Co(II) reduction) were determined after 6 h instead of 24 h (Table 3). As observed for different cobalt(III)

Table 3
Conversion (%) for the reaction between complexes **1** and **2** and ascorbic acid (AA) using different atmospheric conditions (nd: not determined).

Atmosphere	Time	Complex **1**		Complex **2**	
		pH 6.2	pH 7.4	pH 6.2	pH 7.4
Argon	24 h	nd	69	83	84
Argon		19	31	43	69
Air	6 h	6	15	24	39
O_2 sat.		0	4	0	6

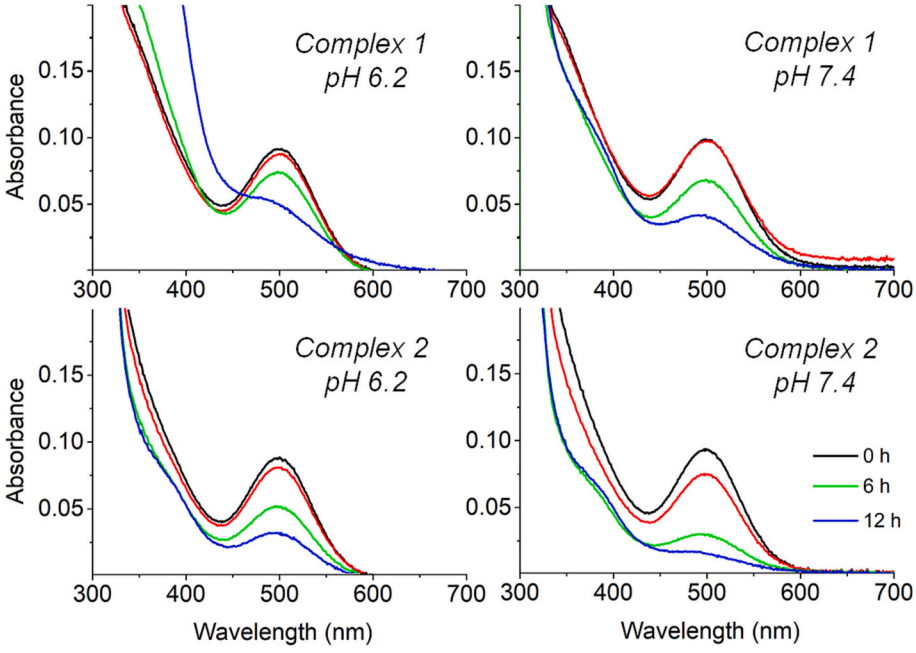

Fig. 5. Reaction between complex **1** and **2** and ascorbic acid (10-fold excess) in PBS (10% DMSO) at pH 6.2 and 7.4 at 37°C under argon, followed by UV–Vis spectroscopy during 12 h.

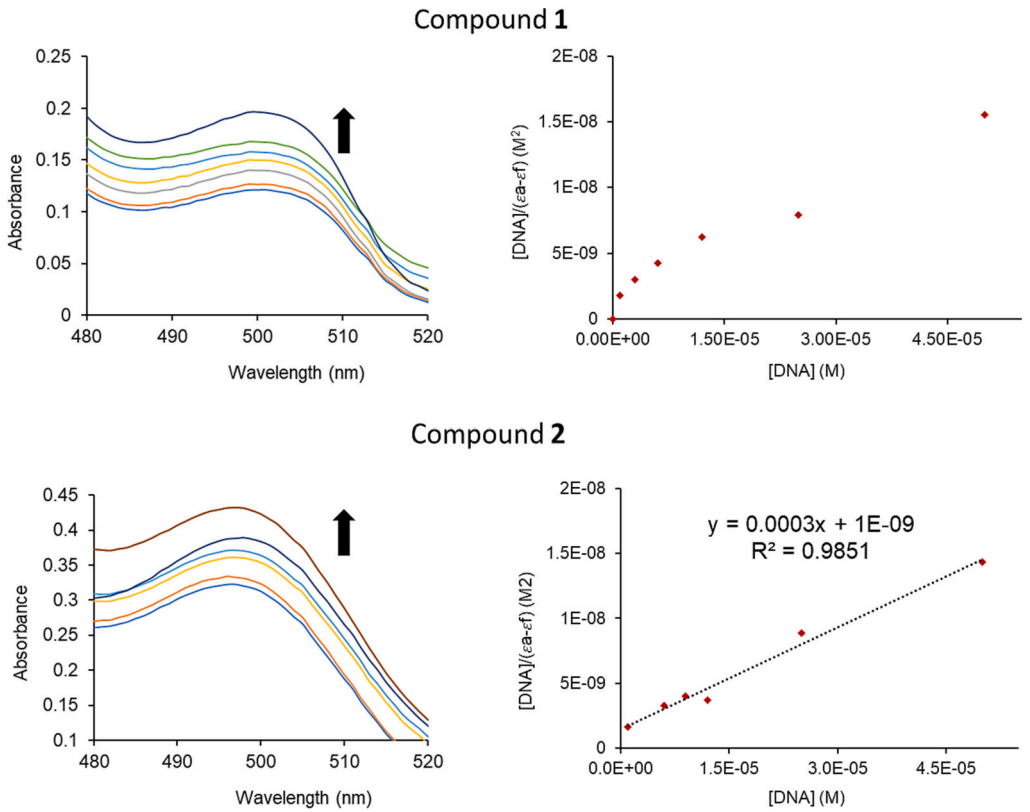

Fig. 6. Absorption spectra of 25 μM solutions of **1** (top) and **2** (bottom), in the presence of increasing amounts of ct-DNA (0–100 μM). The arrows show the intensity change upon increase of [ct-DNA]. The spectra were recorded in cacodylate–NaCl buffer (pH 7.3) after incubation at 37°C for 24 h.

complexes [16], the release of the β-ketoester ligand is hampered by dioxygen (Table 3 and Figs. S14–S21). The pH effect may be associated to the amount of deprotonated form of AA (ascorbate) [16]. It can be pointed out that interesting results were also obtained at pH 6.2 for cobalt(III)-esculetin complexes, and the releasing of the ligand is accompanied by the generation of $[Co(py_2en)(OH)(H_2O)]^+$ species [15,34].

3.5. Binding studies with DNA

The stability of both complexes in cacodylate–NaCl buffer containing 1% DMSO was first verified (Fig. S22). Subsequently, the possible mode (s) of interaction of **1** and **2** with DNA was investigated using various techniques.

3.5.1. UV–Visible spectroscopy

UV–Visible spectra of **1** and **2** were recorded after incubation with increasing amounts of ct-DNA at 37°C for 24 h. Unlike with some cobalt (III)-acac complexes [46], slight hyperchromic effects without wavelength shifts were observed for **1** and **2** upon the addition of DNA (Fig. 6). These features suggest the occurrence of electrostatic or groove-binding interactions between the metal complexes and the biomolecule. Only the data for compound **2** could be fitted to Eq. 1, which yielded a binding constant (K_b) value of 3×10^6 M^{-1}. This value is higher than those found for other related cobalt(III) complexes [46,54].

3.5.2. Viscosity assay

Viscosity measurements may help to determine the way in which a molecule interacts with DNA [55]. Intercalating molecules like thiazole orange, ethidium bromide and chloroquine increase DNA viscosity, as the result of the lengthening of the DNA helix due to base-pair separation. Compounds that strongly bind to DNA, such as cisplatin, give rise to a decrease of viscosity, owing to a shortening of the DNA length. The absence of changes in DNA viscosity can be justified by the lack of or weak interactions between the compound and the biomolecule; for instance, groove or electrostatic interactions may not affect DNA viscosity. As observed in Fig. 7, there are no significant changes in the viscosity profile, thus indicating the occurrence of at best weak interactions between DNA and complexes **1** and **2**.

3.5.3. Circular dichroism

Circular dichroism (CD) was also used to study the interaction of **1** and **2** with DNA; indeed, the interaction of these compounds may cause conformational changes in the chiral biomolecule, which will be reflected by alterations of the CD spectra [56,57]. Spectra of ct-DNA in the presence of **1** and **2** at different complex-to-DNA molar ratios (0.0, 0.2, 0.6 and 1.0) were recorded after 1 h of incubation at 37°C. No significant changes were observed [58], indicating that these cobalt complexes cannot significantly affect the secondary structure of ct-DNA. Most likely, **1** and **2** interact mainly through electrostatic interactions with the double helix (Figs. 7 and S23). These CD data agree with those obtained previously.

3.5.4. Displacement assays with two DNA-binding dyes

Competitive DNA-binding studies with ethidium bromide (EB) were performed to obtain information about the type of interaction between **1** and **2** and the biomolecule. EB is a DNA-intercalating agent that emits strongly at 610 nm when it intercalates between nucleobase pairs; its displacement from DNA by an external competitor thus results in fluorescence quenching. The spectral data obtained indicate that these complexes do not act as intercalators, since no fluorescence quenching was observed (Figs. S24 and S25). Studies using Hoechst 33258 were then carried out. Hoechst is a fluorescent probe that binds in the minor groove of DNA, leading to an emission centered at 460 nm. The results achieved show that both complexes can displace this groove-binding molecule (Figs. 7 and S26).

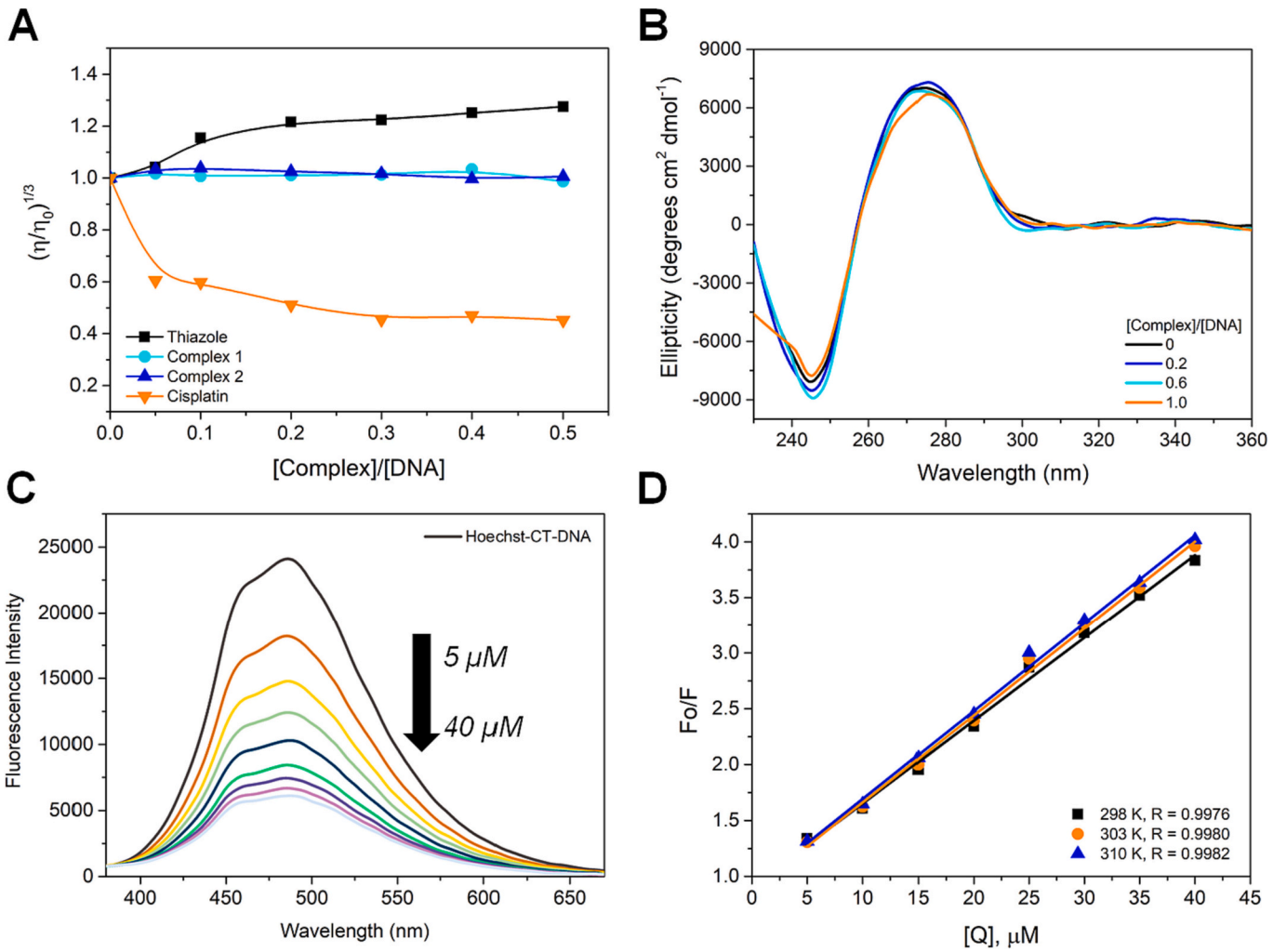

Fig. 7. Binding studies with DNA: (A) Effect of increasing concentrations of **1** and **2**, thiazole orange and cisplatin on the relative viscosity of ct-DNA at 25°C. (B) CD spectra of ct-DNA (100 μM) in the absence and presence of **1** at different complex-to-DNA molar ratios. (C) Fluorescence emission spectra of the DNA–Hoechst complex in the absence and presence of increasing amounts of **1**, [Hoechst] = 5 μM, [DNA] = 100 μM, [Complex] = 5–40 μM, λ_{exc} = 343 nm. (D) Stern-Volmer plot, Q = complex 1.

Table 4
K_{sv} and K_b values and thermodynamic parameters for $[Co^{III}(L1)(py_2en)](ClO_4)_2$ (**1**) and $[Co^{III}(L2)(py_2en)](ClO_4)_2$ (**2**).

Complex	T (K)	K_{sv}	K_b	ΔH (KJ/mol)	ΔS (J/K mol)	ΔG (J/K mol)
1	298	7.41 ± 0.09 × 10^4	1.33 ± 0.05 × 10^5	−66.39	−118.51	−29.24
	303	7.41 ± 0.03 × 10^4	1.90 ± 0.06 × 10^5			−30.49
	310	7.88 ± 0.01 × 10^4	2.13 ± 0.05 × 10^5			−31.56
2	298	7.40 ± 0.08 × 10^4	1.78 ± 0.07 × 10^5	−65.83	−115.51	−29.84
	303	7.69 ± 0.13 × 10^4	1.88 ± 0.18 × 10^5			−30.58
	310	7.92 ± 0.13 × 10^4	2.40 ± 0.20 × 10^5			−31.92

The quenching process was evaluated using the Stern-Volmer equation (Fig. 7 and Table 4). The results show that K_{sv} increases with the temperature, hence indicating that a dynamic process is taking place [59–61]. The thermodynamic parameters, ΔH, ΔS and ΔG were determined for both complexes (Table 4). The negative values obtained for ΔH and ΔS suggest the existence of van der Waals interactions between the complexes and the biomolecule [69–61]; moreover, the observed ΔG values are indicative of a spontaneous process.

3.5.5. Agarose gel electrophoresis

The potential interacting or/and cleaving properties of **1** and **2** were investigated by agarose gel electrophoresis using pBR322 DNA. Different forms of the plasmid can be observed in a gel as the consequence of their distinct electrophoretic mobilities: supercoiled DNA (Form I), which is compact, migrates faster on the gel; open circular DNA (Form II) resulting from a single-strand scission, presents a lower migration rate; linear DNA (Form III), generated when both strands are cleaved, can be observed between Forms I and II. The gel electrophoresis images obtained for complexes **1** and **2** using the conditions described in the "Experimental section", treated with various reducing agents (AA (**A**), GSH (**B**), TCEP (**C**)) and increasing concentrations of the complexes (from 5 to 50 μM) are displayed in Fig. 8. The electrophoretic results indicate that **1** and **2** (lanes 9–14) do not significantly alter the biomolecule (lanes 6, 9, 12 and 15), as already observed with other

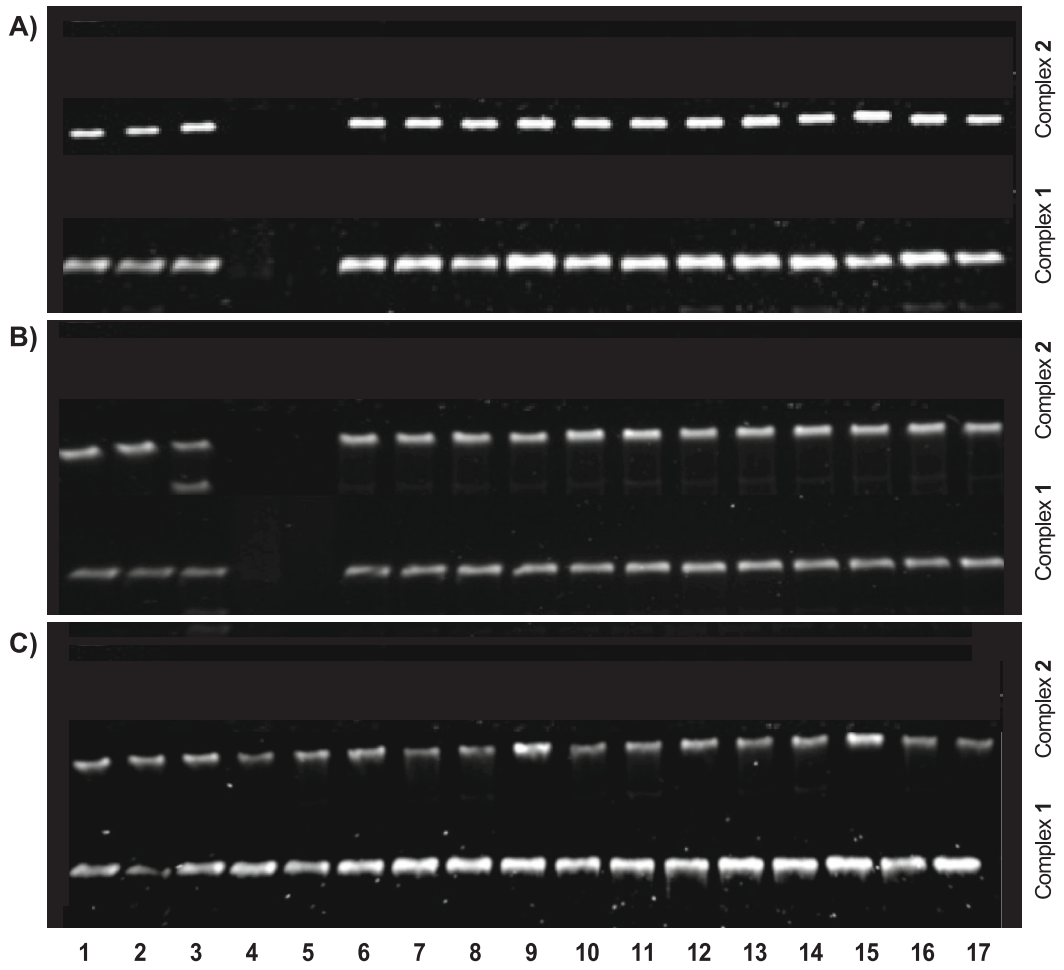

Fig. 8. Agarose gel electrophoresis images of 15 μM_{bp} pBR322 DNA incubated for 1.5 h at 37°C with increasing concentrations of the cobalt(III) complexes in the absence and in the presence of a reducing agent (RA): 100 μM AA (**A**), 150 μM GSH (**B**) and 1 mM TCEP (**C**). In all cases, lanes 1, 2, 3, 4 and 5 correspond to DNA control, DNA control + RA, Cuphen (5 μM), Cuphen (5 μM) + RA and Cuphen (5 μM) + RA with pre-incubation, respectively. Lanes 6–17 correspond to samples treated with complexes **1** (Top) and **2** (Down). Lanes 6, 9, 12 and 15 correspond to DNA-complex samples with increasing complex concentrations (5, 10, 25, 50 μM); Lanes 7, 10, 13 and 16 correspond to DNA-complex samples with added RA; Lanes 8, 11, 14 and 17 correspond to complex samples that were first pre-incubated with RA before DNA addition.

techniques (see above) that indicated that both complexes were weakly interacting with DNA. The use of a reducing agent, namely AA, GSH or TCEP did not lead to any changes of the electrophoretic mobility of the plasmid DNA (lanes 7–8, 10–11, 13–14 and 16–17) (Fig. 8), thus indicating that both the cobalt(II) species and the freed β-ketoester ligand generated upon cobalt(III) reduction are not (strongly) interacting with the DNA.

4. Conclusions

Two new cobalt(III)-β-ketoester complexes were prepared and their potential use as carriers of bioactive molecules to be released under hypoxic conditions was investigated. Although the Co^{3+}/Co^{2+} redox potential in PBS was found to be more positive than the ideal range reported for bioreduction under a hypoxic environment (−0.2 to −0.4 V *vs.* SHE), complex **2** appeared to be a possible candidate as a targeted-delivery carrier. Indeed, reactivity studies using a reducing agent, *i.e.* ascorbic acid, to mimic a hypoxic tumor microenvironment indicated that complex **2** presents a significantly higher degree of dissociation of the β-ketoester ligands upon Co(III)-to-Co(II) reduction. The results allow us to envisage the utilization of such β-ketoester-cobalt-based compounds as redox-active drug carriers. Thus, the next steps to be investigated include a fine-tuning of the release properties by adjusting the electronic properties of the ligands, introducing electron donating and/or electron-withdrawing substituents on both the N_4 tetradentate ligand and the β-ketoesters. Moreover, the possible use of known β-ketoesters-containing drugs and their redox-induced release could be investigated.

CRediT authorship contribution statement

Marcos V. Palmeira-Mello: Methodology, Investigation, Validation, Formal analysis, Data curation, Writing – original draft. **Ana B. Caballero:** Conceptualization, Methodology, Writing – review & editing. **Piedad Herrera-Ramírez:** Investigation, Validation. **Analu R. Costa:** Investigation, Validation. **Savyo S. Santana:** Investigation, Validation. **Guilherme P. Guedes:** Investigation, Validation, Formal analysis, Resources. **Amparo Caubet:** Writing – review & editing, Supervision. **Alzir Azevedo Batista:** Resources, Writing – review & editing, Supervision. **Patrick Gamez:** Conceptualization, Resources, Writing – review & editing, Supervision, Project administration, Funding acquisition. **Mauricio Lanznaster:** Conceptualization, Resources, Writing – review & editing, Supervision, Project administration, Funding acquisition.

Declaration of Competing Interest

The authors declare no conflicts of interest.

Data availability

Data will be made available on request.

Acknowledgements

This study was financed in part by the Coordenação de Aperfeiçoamento de Pessoal de Nível Superior – Brazil (CAPES) – Finance Code 001 (PDSE, Process 88881.187405/2018-01) and São Paulo State Research Support Foundation (FAPESP, Process 2021/01787-0). We thank LAME (Laboratório Multiusuário de Espectroscopia), LaReMN (Laboratório Multiusuário de Ressonância Magnética Nuclear) and LAMEM (Laboratório Multiusuário de Espectrometria de Massas) of Universidade Federal Fluminense for the use of their facilities. Financial support from the Spanish Ministerio de Ciencia e Innovación (Projects PID2020-115537RB-I00 and RED2018-102471-T; MCIN/ AEI /10.13039/501100011033) is kindly acknowledged. M. Lanznaster thanks CNPq (303258/2019-5, 307928/2022-5) and FAPERJ (E-26/010.101123/2018, SEI-260003/001190/2020) for their financial support.

Appendix A. Supplementary data

Supplementary data to this article can be found online at https://doi.org/10.1016/j.jinorgbio.2023.112345.

References

[1] J.M. Brown, W.R. Wilson, Nat. Rev. Cancer 4 (2004) 437–447, https://doi.org/10.1038/nrc1367.
[2] Z. Chen, F. Han, Y. Du, H. Shi, W. Zhou, Signal Transduct. Target. Ther. 8 (2023) 70, https://doi.org/10.1038/s41392-023-01332-8.
[3] A. Bogdanov, A. Bogdanov, V. Chubenko, N. Volkov, F. Moiseenko, V. Moiseyenko, Front. Oncol. 12 (2022) 979154, https://doi.org/10.3389/fonc.2022.979154.
[4] N. Graf, S.J. Lippard, Adv. Drug Deliv. Rev. 64 (2012) 993–1004, https://doi.org/10.1016/j.addr.2012.01.007.
[5] Y. Li, L. Zhao, X.-F. Li, Front. Oncol. 11 (2021) 700407, https://doi.org/10.3389/fonc.2021.700407.
[6] P. Zhang, P.J. Sadler, Eur. J. Inorg. Chem. (2017) 1541–1548, https://doi.org/10.1002/ejic.201600908.
[7] A.K. Renfrew, Metallomics 6 (2014) 1324–1335, https://doi.org/10.1039/C4MT00069B.
[8] C.R. Munteanu, K. Suntharalingam, Dalton Trans. 44 (2015) 13796–13808, https://doi.org/10.1039/c5dt02101d.
[9] F.L.S. Bustamante, F.S. Miranda, F.A.V. Castro, J.A.L.C. Resende, M.D. Pereira, M. Lanznaster, J. Inorg. Biochem. 132 (2014) 37–44, https://doi.org/10.1016/j.jinorgbio.2013.11.007.
[10] I.C.A. de Souza, L.V. Faro, C.B. Pinheiro, D.T.G. Gonzaga, F.C. Silva, V.F. Ferreira, F.S. Miranda, M. Scarpellini, M. Lanznaster, Dalton Trans. 45 (2016) 13671–13674, https://doi.org/10.1039/C6DT02456D.
[11] M.V.P. Mello, G. Cebrián-Torrejón, J.R. Pereira, C.S. Moreira, C.B.S.M.R. Gomes, D. R. Rocha, E.M.S. Fagundes, G.B. Ferreira, M. Lanznaster, J. Inorg. Biochem. 199 (2019) 110756, https://doi.org/10.1016/j.jinorgbio.2019.110756.
[12] A.F.M. Silva, M.V.P. Mello, J.G. Gómez, G.B. Ferreira, M. Lanznaster, Eur. J. Inorg. Chem. (2019) 1784–1791, https://doi.org/10.1002/ejic.201801550.
[13] B.M. Pires, L.C. Giacomin, F.A.V. Castro, A.S. Cavalcanti, M.D. Pereira, A. J. Bortoluzzi, R.B. Faria, M. Scarpellini, J. Inorg. Biochem. 157 (2016) 104–113, https://doi.org/10.1016/j.jinorgbio.2016.01.024.
[14] E.S. Areas, J.L.A. Paiva, F.V. Ribeiro, T.M. Pereira, A.E. Kummerle, G.P. Guedes, A. C.C. Nascimento, F.S. Miranda, A.P. Neves, Eur. J. Inorg. Chem. 37 (2019) 4031–4039, https://doi.org/10.1002/ejic.201900734.
[15] M.V. Palmeira-Mello, A.B. Caballero, J.M. Ribeiro, E.M. Souza-Fagundes, P. Gamez, M. Lanznaster, J. Inorg. Biochem. 211 (2020) 111211, https://doi.org/10.1016/j.jinorgbio.2020.111211.
[16] I.C.A. de Souza, S.S. Santana, J.G. Gomez, G. Guedes, J. Madureira, S.M.D. O. Quintal, M. Lanznaster, Dalton Trans. 49 (2020) 16425–16439, https://doi.org/10.1039/D0DT01389G.
[17] J.Y.-C. Chang, R.J. Stevenson, G.-L. Lu, P.J. Brothers, G.R. Clark, W.A. Denny, D. C. Ware, Dalton Trans. 39 (2010) 11535–11550, https://doi.org/10.1039/C0DT01142H.
[18] M. Mathuber, M. Gutmann, M. la Franca, P. Vician, A. Laemmerer, P. Moser, B. K. Keppler, W. Berger, C.R. Kowol, Inorg. Chem. Front. 8 (2021) 2468, https://doi.org/10.1039/D1QI00211B.
[19] A. Pana, P. Kundu, S. Paul, P. Kondaiah, A.R. Chakravarty, Inorg. Chem. 61 (18) (2022) 6837–6851, https://doi.org/10.1021/acs.inorgchem.2c00150.
[20] M. Caban, B. Koblmueller, D. Groza, H.H. Schueffl, A. Terenzi, A. Tolios, T. Mohr, M. Mathuber, K. Kryeziu, C. Jaunecker, C. Pirker, B.K. Keppler, W. Berger, C. R. Kowol, P. Heffeter, Cancer Lett. 565 (2023) 216237, https://doi.org/10.1016/j.canlet.2023.216237.
[21] P.D. Bonnitcha, B.J. Kim, R.K. Hocking, J.K. Clegg, P. Turner, S.M. Neville, T. W. Hambley, Dalton Trans. (2012) 11293, https://doi.org/10.1039/c2dt30727h.
[22] A. Glenister, C.K.J. Chen, E.M. Tondl, D. Paterson, T.W. Hambley, A.K. Renfrew, Metallomics 9 (2017) 699–705, https://doi.org/10.1039/c6mt00275g.
[23] A.K. Renfrew, N.S. Bryce, T.W. Hambley, Chem. Sci. 4 (2013) 3731–3739, https://doi.org/10.1039/c3sc51530c.
[24] E.S. O'Neill, A. Kaur, D.P. Bishop, D. Shishmarev, P.W. Kuchel, S.M. Grieve, G. A. Figtree, A.K. Renfrew, P.D. Bonnitcha, E.J. New, Inorg. Chem. (2017) 9860–9868, https://doi.org/10.1021/acs.inorgchem.7b01368.
[25] M. Mathuber, H. Schueffl, O. Dömötör, C. Karnthaler, E.A. Enyedy, P. Heffeter, B. K. Keppler, C.R. Kowol, Inorg. Chem. 59 (23) (2020) 17794–17810, https://doi.org/10.1021/acs.inorgchem.0c03083.
[26] S.S. Santana, M. Lanznaster, Inorg. Chem. Commun. 15 (2023) 110810, https://doi.org/10.1016/j.inoche.2023.110810.
[27] K. Beaumont, R. Webster, I. Gardner, K. Dack, Curr. Drug Metab. (2003) 461–485, https://doi.org/10.2174/1389200033489253.
[28] J. Rautio, H. Kumpulainen, T. Heimbach, R. Oliyai, D. Oh, T. Jarvinen, J. Savolainen, Nat. Rev. Drug Discov. (2008) 255–270, https://doi.org/10.1038/nrd2468.
[29] C.A. McGoldrick, Y.-L. Jiang, V. Paromov, M. Brannon, K. Krishnan, W.L. Stone, BMC Cancer 14 (2014) 77, https://doi.org/10.1186/1471-2407-14-77.
[30] C. Hureau, G. Blondin, M.F. Charlot, C. Philouze, M. Nierlich, M. Césario, E. Anxolabéhère-Mallart, Inorg. Chem. (2005) 3669–3683, https://doi.org/10.1021/ic050243y.
[31] R.N. Firmo, I.C.A. de Souza, F.S. Miranda, C.B. Pinheiro, J.A.L.C. Resende, M. Lanznaster, Polyhedron 117 (2016) 604–611, https://doi.org/10.1016/j.poly.2016.06.022.
[32] R. Gagne, C. Koval, G. Licenski, Inorg. Chem. 19 (1980) 2854–2855, https://doi.org/10.1021/ic50211a080.
[33] P.T. Kissinger, Laboratory Techniques in Electroanalytical Chemistry, second ed., Marcel Dekker Inc., New York, 1996.
[34] R.C. Batista, F.S. Miranda, C.B. Pinheiro, M. Lanznaster, Eur. J. Inorg. Chem. (2018) 612–616, https://doi.org/10.1002/ejic.20170125.
[35] Bruker, APEX3, Bruker AXS Inc., Madison, Wisconsin, USA, 2012.
[36] Bruker, SAINT, Bruker AXS Inc., Madison, Wisconsin, USA, 2012.
[37] Bruker, SADABS, Bruker AXS Inc., Madison, Wisconsin, USA, 2001.
[38] G.M. Sheldrick, Acta Cryst C71 (2015) 3–8.
[39] C.F. Macrae, P.R. Edgington, P. McCabe, E. Pidcock, G.P. Shields, R. Taylor, M. Towler, J. van de Streek, J. Appl. Crystallogr. 39 (2006) 453–457.
[40] J. Marmur, P. Doty, J. Mol. Biol. 5 (1962) 109–118, https://doi.org/10.1016/S0022-2836(62)80066-7.
[41] F.C. Savariz, M.A. Foglio, A.L.T.G. Ruiz, W.F. Costa, M.M. Silva, J.C.C. Santos, I. M. Figueiredo, E. Meyer, J.E. Carvalho, M.H. Sarragiotto, Bioorg. Med. Chem. 22 (2014) 6867–6875, https://doi.org/10.1016/j.bmc.2014.10.031.
[42] T.J.P. McGivern, S. Afsharpour, C.J. Marmion, Inorg. Chim. Acta 472 (2018) 12–39, https://doi.org/10.1016/j.ica.2017.08.043.
[43] K. Nakamoto, Infrared and Raman Spectra of Inorganic and Coordination Compounds, 4rd ed., John Wiley, New York, 1986.
[44] A.F.M. da Silva, R.U. Vital, D.L. Martins, D.R. da Rocha, G.B. Ferreira, J.A.L. C. Resende, M. Lanznaster, New J. Chem. 41 (2017) 14960–14965, https://doi.org/10.1039/c7nj03072j.
[45] R. Liu, P.H. van Rooyen, J. Conradie, Inorg. Chim. Acta 447 (2016) 59–65, https://doi.org/10.1016/j.ica.2016.03.019.
[46] V. Thamilarasan, N. Sengottuvelan, A. Sudha, P. Srinivasan, G. Chakkaravarthi, J. Photochem. Photobiol. B 162 (2016) 558–569, https://doi.org/10.1016/j.jphotobiol.2016.06.024.
[47] T. Sarkar, S. Banerjee, A. Hussain, RSC Adv. 5 (2015) 16641, https://doi.org/10.1039/c4ra17314g.
[48] A.F.M. da Silva, M.V.P. de Mello, J.G. Gómez, G.B. Ferreira, M. Lanznaster, Eur. J. Inorg. Chem. 13 (2019) 1784–1791, https://doi.org/10.1002/ejic.201801550.
[49] F.L.S. Bustamante, F.S. Miranda, F.A.V. Castro, J.A.L.C. Resende, M.D. Pereira, M. Lanznaster, Inorg. Biochem. 132 (2014) 37–44, https://doi.org/10.1016/j.jinorgbio.2013.11.007.
[50] M. Gümüs, Y. Sert, S. Ozdemir, H. Gokce, I. Kani, I. Koca, J. Mol. Struct. 1167 (2018) 280–293, https://doi.org/10.1016/j.molstruc.2018.05.008.
[51] A.M. Sargeson, G.H. Searle, Inorg. Chem. 6 (1967) 787–796, https://doi.org/10.1021/ic50050a029.
[52] J.G. Gibson, E.D. McKenzie, J. Chem. Soc. A (1971) 1666–1683, https://doi.org/10.1039/J19710001666.
[53] C.M. Coates, K. Hagan, C.A. Mitchell, J.D. Gorden, C.R. Goldsmith, Dalton Trans. 40 (2011) 4048–4058, https://doi.org/10.1039/C0DT01556C.
[54] S. Mondal, B. Pakhira, A.J. Blake, M.G.B. Drew, S.K. Chattopadhyay, Polyhedron 117 (2016) 327–337, https://doi.org/10.1016/j.poly.2016.05.052.
[55] A. Kellett, Z. Molphy, C. Slator, V. McKee, N.P. Farrell, Chem. Soc. Rev. 48 (2019) 971, https://doi.org/10.1039/c8cs00157j.
[56] S.R. Martin, M.J. Schilstra, Methods Cell Biol. 84 (2008) 263–293, https://doi.org/10.1016/S0091-679X(07)84010-6.
[57] B. Nordén, A. Rodger, T. Dafforn, Linear and Circular Dichroism: A Textbook on Polarized-Light Spectroscopy, RSC Publishing, Cambrigde, 2010.
[58] M.V. Palmeira-Mello, A.B. Caballero, A. Lopez-Espinar, G.P. Guedes, A. Caubet, A. M.T. de Souza, M. Lanznaster, P. Gamez, J. Biol. Inorg. Chem. 26 (2021) 727–740, https://doi.org/10.1007/s00775-021-01888-2.

[59] P. Sathyadevi, P. Krishnamoorthy, R.R. Butorac, A.H. Cowley, N.S. Bhuvanesh, N. Dharmaraj, Dalton Trans. 40 (2011) 9690–9702, https://doi.org/10.1039/C1DT10767D.

[60] H. Yang, P. Tang, B. Tang, Y. Huang, X. Xiong, H. Li, RSC Adv. 7 (2017) 10242, https://doi.org/10.1039/c6ra28213j.

[61] P.D. Ross, S. Subramanian, Biochemistry 26 (1981) 3096–3102, https://doi.org/10.1021/bi00514a017.